Journal of Sound and Vibration (1998) **211**(2), 157–177

PULSE INPUT SEQUENCES FOR RESIDUAL VIBRATION REDUCTION

C. L. Teo, C. J. Ong and M. Xu

Department of Mechanical and Production Engineering, *National University of Singapore*, 10 *Kent Ridge Crescent*, *Singapore* 119260

(*Received* 2 *January* 1997, *and in final form* 9 *September* 1997)

Preshaping of the input is a well known technique to reduce the vibration in a flexible structure. In this paper, inputs in the form of pulse sequences that are able to reduce the residual vibration in overhead crane are presented. If the exact natural frequency and damping ratio of the system are known, then the residual vibration can be eliminated completely. However, additional constraints can be imposed to incorporate some robustness in the system to variations in the natural frequency and damping ratio for practical implementation. Simulation results and experimental tests show that the inputs developed here are effective in moving the system with no or little residual vibration. In addition, the suggested inputs with robustness incorporated show marked insensitivity to errors in natural frequency and damping ratio estimates.

1. INTRODUCTION

Vibration is a serious problem in mechanical systems that are required to perform precise motion in the presence of structural flexibility. Examples of such systems range from the positioning of a disk drive's head to large space structures, flexible manipulators and overhead cranes. In most cases, the residual vibration at the end of a move is the most detrimental and the extent of the residual vibration limits the performance of the system. The effective use of such systems can only be achieved when such vibration can be properly handled. As a result, there is active research interest in finding methods that will eliminate vibration for a variety of mechanical and structural systems.

Traditional closed loop feedback can be used to reduce end-point vibration (see, for example, [1, 2]). The closed loop system will then benefit from the inherent advantages of feedback, such as insensitivity to parameter variations, noise attenuation and disturbance rejection. However, such a feedback system can be difficult to implement in practice, as it requires reliable sensor information for feedback. Such sensor information may not be so easily available. For example, in the overhead crane problem, it is not a trivial task (nor practical) to devise a sensor to measure the position at the end-point. Another approach is input command shaping, in which the input is preshaped such that the resulting residual vibration is reduced or eliminated. These methods are popular in industry because they are relatively simple to implement and do not require additional sensor information. In some cases, it is possible to use the preshaped input together with closed loop feedback strategies to enjoy the benefits of both systems [3, 4].

Input command shaping involves altering the shape of the actuator's command so that residual vibration is reduced. Such a command shaping technique was first introduced in

0022–460X/98/120157 + 21 $25.00/0/sv971360

the work of Smith [5, 6], through his Posicast control scheme. In that scheme, a step input is divided into two smaller steps, with the second step delayed in time. The idea is to apply the second step so as to cancel the vibration induced by the first. If the steps are chosen properly, the resulting system will have considerably reduced vibration. However, the scheme was not considered to be suitably robust for practical application.

Many researchers have worked in this area. Aspinwall [9] shaped the forcing function with a sine series expression to minimize the residual response of a flexible structure over a band of frequencies. Farrenkof [7] developed profiles that minimize a structural excitation criterion for a spacecraft with flexible appendages. Swigert [8] used a performance index that minimizes the sensitivity of vibration to error in plant parameter estimates. Meckl and Kinceler [10] considered ramped sinusoids as basis functions, so as to minimize excitation over a range of frequencies surrounding the system natural frequency. The coefficients of the basis functions are chosen to minimize the difference between the ramped sinusoids and the rigid body minimum time solution. Jones *et al*. [11] applied a constant acceleration profile to damp oscillations in objects transported by an overhead crane. By delaying a constant acceleration input by a certain time, the transported object is then able to move during the constant velocity stage without vibration. Then the same strategy is applied to decelerate the transported object so that the residual vibration can be reduced. Although this method can be applied to systems with large amplitudes of oscillation, it can only be used on single mode systems without damping, and may not be suitably robust for practical implementation.

Singer and Seering [12] developed an elegant input shaper using impulse sequences to cancel the residual vibration. The impulse sequence is convolved with the user's desired input to produce a shaped command for the system. The resulting shaped command has the same vibration reduction properties as the impulse sequence. In their method, the natural frequency and damping ratio of the system need to be known exactly, but additional impulses can be introduced to reduce the sensitivity of these parameters.

In this paper, a series of pulse sequences are proposed that can produce damped motion and reduce the residual vibration. The user has the choice of pulse sequences to select, depending on the requirements. Some pulse sequences possess robustness to variations in the parameters of the system. While no guarantee of time optimality is made, the results (as measured by the residual vibrations and the time taken) compare well with existing methods. The suggested input profiles are easy to design and implement and, in fact, could also be used as the initial guess for any optimal solution of the problem.

The paper is organized as follows. A model of an overhead crane system is presented in section 2. The input forcing function and the conditions for zero residual vibration are shown in section 3. On the basis of sections 2 and 3, a two-pulse sequence, a four-pulse sequence and a six-pulse sequence are developed in section 4. A brief description of the impulse shaper method of reference [12] is given in section 5. Simulation results and discussion for the system are presented in section 6. The experimental set-up and results are shown in section 7. The conclusions are presented in section 8.

Notation. In the derivation below and the rest of this paper, the function $1(t - t_i)$ is equal to 1 for $t \geqslant t_i$ and 0 otherwise; the function $\text{int}(x)$ means to take the integer part of x; for example, $\text{int}(2{\cdot}67) = 2$; an asterisk denotes convolution; and all the variables beginning with L are positive integers. In this paper, a_{max} and v_{max} denote the maximum acceleration and velocity attainable by the rigid body system, and z is the desired rigid body motion. With this assumption, the inequality $z \geqslant v_{max}^2 / a_{max}$ can always be satisfied.

2. SYSTEM MODEL

The pulse sequence developed here can be used to reduce the residual vibration of any time-invariant second order linear system. As a specific example, a model of an overhead crane as shown in Figure 1 is considered. It consists of a motorized platform moving in the horizontal direction with a cable and point load attached. The equations of motion governing the system are given by

$$(M + m)\ddot{x}_M - ml(\ddot{\theta}\cos\theta - \dot{\theta}^2 \sin\theta) = F, \tag{2.1}$$

$$\ddot{\theta} + \frac{g}{l}\sin\theta = \frac{\ddot{x}_M}{l}\cos\theta, \tag{2.2}$$

where M and m are the masses of the cart and the load respectively, $x_M(t)$ is the horizontal displacement of the platform, l is the length of the rope, F is the force on the cart and $\theta(t)$ is the angular displacement. Equations (2.1) and (2.2) are non-linear coupled equations. The approach taken here is to consider only equation (2.2) and to treat the acceleration, $\ddot{x}_M(t)$, of the cart as the input. For a desired acceleration profile, $\theta(t)$, $\dot{\theta}(t)$ and $\ddot{\theta}(t)$ can be obtained numerically from equation (2.2) and hence $F(t)$ can be found from equation (2.1).

Using this approach, and assuming the angular displacement of the pendulum to be small so that standard linearization of equation (2.2) is possible, the equation of motion becomes

$$\ddot{\theta} + \frac{g}{l}\theta = \frac{\ddot{x}_M}{l}. \tag{2.3}$$

With the damping effect incorporated, equation (2.3) can be written as

$$\ddot{\theta} + 2\xi\omega_n\dot{\theta} + \omega_n^2\theta = \ddot{x}_M/l, \tag{2.4}$$

where ξ is the damping coefficient and $\omega_n = \sqrt{g/l}$ is the natural frequency of the system. Since θ is assumed to be small such that $\Delta x = l\sin\theta = l\theta$, equation (2.4) can also be written as

$$\Delta\ddot{x} + 2\xi\omega_n\Delta\dot{x} + \omega_n^2\Delta x = Du, \tag{2.5}$$

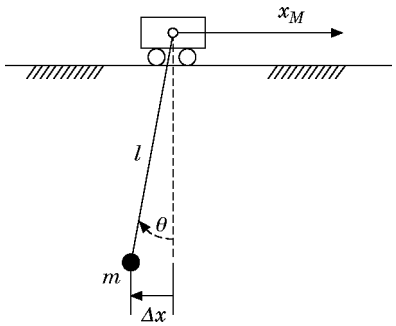

Figure 1. The model of an overhead crane.

where D is a constant of the system. Equation (2.5) is the general equation of motion of a time-invariant second order linear system excited by a forcing function $u(t)$.

The basic problem now is to design an input profile that will move the cart from one operating point to another in the shortest time possible with zero residual vibration. The system is assumed to be at rest initially. In addition, it is also desirable that there should be little or no vibration during the movement.

3. INPUT FORCING FUNCTIONS AND SUPPRESSION OF RESIDUAL VIBRATION

In this paper, the cart is assumed to be a computer-controlled unmanned platform, where the comfort of the ride is not a significant factor. Hence, $u(t)$ can be chosen as a non-uniform piecewise step sequences given by

$$u(t) = \ddot{x}_M(t) = \sum_{i=1}^{n} a_i \cdot 1(t - t_i), \tag{3.1}$$

where $t_i > t_{i-1}$, $i = 2, 3, \ldots, n$, and a_i is a constant amplitude. It can be seen later that such a choice of $u(t)$ will lead naturally to a rectangular or "bang–bang" forcing function, and it is well known that such inputs are time-optimal solutions. Of course, it is also known that such inputs will excite the higher order modes and give rise to a highly oscillatory response, but it will be shown that, by proper selection of the step sequences, the vibration can be reduced substantially.

The response of the time-invariant second order linear system given by equation (2.5) to the step sequence (3.1) can be shown to be

$$\Delta x(t) = \sum_{i=1}^{n} \Delta x_i(t) = \frac{D}{\omega_n^2} \sum_{i=1}^{n} a_i \left\{ 1 - \frac{1}{\sqrt{1-\xi^2}} e^{-\xi\omega_n (t - t_i)} \cos\left[\omega_d (t - t_i) - \delta\right] \right\} \cdot 1(t - t_i) \tag{3.2}$$

where $\delta = \tan^{-1}(\xi/\sqrt{1-\xi^2})$ and $\omega_d = \omega_n \sqrt{1-\xi^2}$ is the damped natural frequency of the system. In particular, the response at the end of the input sequence, i.e., the vibration for $t > t_n$ or residual vibration, is of interest. For all time $t > t_n$, $1(t - t_i) = 1$ and the resulting response is given by

$$\Delta x(t) = \sum_{i=1}^{n} \Delta x_i(t) = \frac{D}{\omega_n^2} \sum_{i=1}^{n} a_i \left\{ 1 - \frac{1}{\sqrt{1-\xi^2}} e^{-\xi\omega_n (t - t_i)} \cos\left[\omega_d (t - t_i) - \delta\right] \right\}. \tag{3.3}$$

In order to achieve zero residual vibration, it is necessary that, for all $t > t_n$,

$$\Delta x(t) = \sum_{i=1}^{n} \Delta x_i(t) = \frac{D}{\omega_n^2} \sum_{i=1}^{n} a_i \left\{ 1 - \frac{1}{\sqrt{1-\xi^2}} e^{-\xi\omega_n (t - t_i)} \cos\left[\omega_d (t - t_i) - \delta\right] \right\} = 0. \tag{3.4}$$

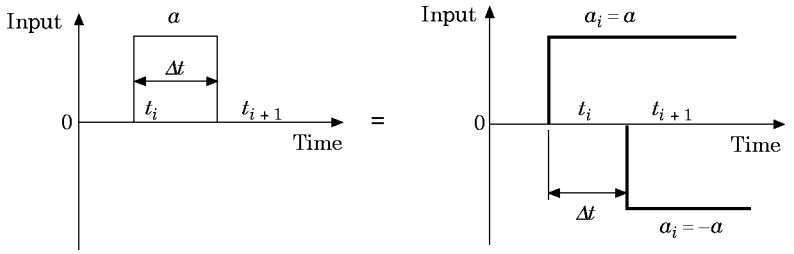

Figure 2. An input pulse.

For equation (3.4) to be true, the following conditions must be satisfied:

$$\sum_{i=1}^{n} a_i = 0, \tag{3.5}$$

$$A_x = -\sum_{i=1}^{n} a_i \, \mathrm{e}^{-\xi\omega_n (t_n - t_i)} \cos \omega_d (t_n - t_i) = 0, \tag{3.6}$$

$$A_y = \sum_{i=1}^{n} a_i \, \mathrm{e}^{-\xi\omega_n (t_n - t_i)} \sin \omega_d (t_n - t_i) = 0. \tag{3.7}$$

Equations (3.5), (3.6) and (3.7) are known as the zero residual vibration constraints, i.e., if these conditions are satisfied, there will be zero residual vibration. Note that these constraints depend on precise knowledge of ω_n and ξ. In order to make the system more robust, and hence less sensitive to variations in the natural frequency of the system, additional constraints are obtained by setting the partial derivatives of equations (3.6) and (3.7) with respect to ω_n to be equal to zero. This means that

$$\frac{\partial A_x}{\partial \omega_n} = \sum_{i=1}^{n} a_i (t_n - t_i) \, \mathrm{e}^{-\xi\omega_n (t_n - t_i)} \{\xi \cos \omega_d (t_n - t_i) + \sqrt{1 - \xi^2} \sin \omega_d (t_n - t_i)\} = 0, \tag{3.8}$$

$$\frac{\partial A_y}{\partial \omega_n} = \sum_{i=1}^{n} a_i (t_n - t_i) \, \mathrm{e}^{-\xi\omega_n (t_n - t_i)} \{-\xi \sin \omega_d (t_n - t_i) + \sqrt{1 - \xi^2} \cos \omega_d (t_n - t_i)\} = 0. \tag{3.9}$$

Similarly, for robustness to variations in the damping ratio, the partial derivatives of equations (3.6) and (3.7) with respect to damping ratio can be found and equated to zero. It turns out that the same relations, equations (3.8) and (3.9), are obtained. This is useful, because it means that when the input sequence is insensitive to error in natural frequency estimates, it is also insensitive to error in damping ratio estimates. Equations (3.8) and (3.9) are known as the robustness conditions.

Constraint (3.5) can be eliminated if the input sequence is chosen as

$$a_{2k} = -a_{2k-1}, \qquad \text{for } k = 1, \ldots, N. \tag{3.10}$$

where $n = 2N$. Such a choice of step sequence will result in a pulse sequence; every two steps constitute a pulse, as shown in the Figure 2. It is easy to show that such a pulse

sequence will automatically satisfy the constraint (3.5). Also, it is assumed that the duration of every pulse in the pulse sequence is the same; i.e.,

$$t_{2k} - t_{2k-1} = \Delta t. \tag{3.11}$$

Therefore, the zero residual vibration constraints *without robustness* in the natural frequency and damping ratio of the system for a pulse sequence input are equations (3.6) and (3.7); the zero residual vibration constraints *with robustness* in the natural frequency and damping ratio of the system for a pulse sequence input are equations (3.6), (3.7), (3.8) and (3.9).

In addition, equations (3.6) and (3.7) are equivalent to

$$A^2 = A_x^2 + A_y^2 = 0, \tag{3.12}$$

while equations (3.8) and (3.9) are equivalent to

$$B = (\partial A_x / \partial \omega_n)^2 + (\partial A_y / \partial \omega_n)^2 = 0. \tag{3.13}$$

In this case, the zero residual vibration constraint without robustness in the natural frequency and damping ratio of the system for a pusle sequence input is equation (3.12), while the zero residual vibration constraints with robustness in the natural frequency and damping ratio of the system for a pulse sequence input are equations (3.12) and (3.13).

4. DESIGN OF PULSE SEQUENCE

In this section, three types of pulse sequences input—namely, the two-pulse, three-pulse and six-pulse sequences—are considered. It will first be shown that the two-pulse sequence can achieve damped motion, and the result is then extended to point-to-point motion with zero residual vibration using the six-pulse sequence. In the analysis, the underlying practical and reasonable assumption is that one would want the system to make full use of its available energy, so that the solution can be near optimal. Hence, it is assumed that the input acceleration should try to reach the maximum acceleration possible for the system. In deciding between possible solutions, it is also assumed that the velocity of the input should be as large as possible in order to minimize the time taken for a move.

4.1. DAMPED MOTION BY A TWO-PULSE SEQUENCE WITHOUT ROBUSTNESS

Consider a two-pulse sequence as shown in Figure 3. It will be shown that such a sequence can be used to achieve *damped motion* without robustness. By damped motion, we mean motion that is free from oscillation. Since the vibration caused by the first pulse will decay by a factor of $e^{-\xi\omega_n t_c}$ after time t_c, in order to cancel the vibration, it is natural to assume that the amplitude of the second pulse is multiplied by a factor of $k_c = e^{-\xi\omega_n t_c}$.

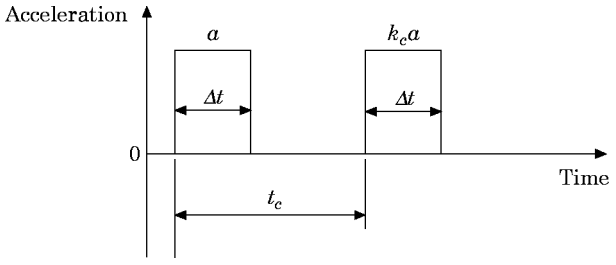

Figure 3. The acceleration profile of the two-pulse sequence for damped motion.

Substituting this pulse sequence into the zero residual vibration constraint (3.12), one obtains

$$A^2 = A_x^2 + A_y^2$$

$$= 4a^2k_c^2 \cos^2 \frac{\omega_d t_c}{2} [e^{-2\xi\omega_n \Delta t} - 2\, e^{-\xi\omega_n \Delta t} \cos(\omega_d \Delta t) + 1]^2 = 0.$$

If $\xi \neq 0$, then $[e^{-2\xi\omega_n \Delta t} - 2\, e^{-\xi\omega_n \Delta t} \cos(\omega_d \Delta t) + 1]^2 \neq 0$, and therefore

$$\cos \frac{\omega_d t_c}{2} = 0,$$

which means that $t_c = (L - 0{\cdot}5)T$ where $T = 2\pi/\omega_d$ and L is an integer. If $\xi = 0$, then $A^2 = 8a^2 \cos^2(\omega_d t_c/2)[1 - \cos(\omega_d \Delta t)]^2 = 0$, and so (a) $\cos(\omega_d t_c/2) = 0$, which means that $t_c = (L - 0{\cdot}5)T$, or (b) $1 - \cos(\omega_d \Delta t) = 0$, which means that $\Delta t = L'T$ where L' is an integer. Therefore, the zero vibration condition for the two-pulse sequence is

$$t_c = (L - 0{\cdot}5)T \qquad \text{when } \xi \neq 0, \tag{4.1}$$

or

$$t_c = (L - 0{\cdot}5)T \qquad \text{or } \Delta t = L'T \qquad \text{when } \xi = 0. \tag{4.2}$$

This means that, for this pulse sequence, damped motion can be obtained either by varying the time delay for the second pulse or, when $\xi = 0$, by varying the width of the pulse. However, if one is to vary the width of the pulse, then it is possible to obtain very narrow pulses and the system may not reach its maximum velocity. Hence the condition $\Delta t = L'T$ is deemed too restrictive to be useful in practice and is thus ignored. Instead, the condition $t_c = (L - 0{\cdot}5)T$ may be more useful.

To see if the latter expression for t_c is able to satisfy the robustness constraint (3.13), equation (4.1) is substituted into equation (3.13), to give

$$B = (\partial A_x/\partial\omega_n)^2 + (\partial A_y/\partial\omega_n)^2$$

$$= k_c^2 a^2 (L - 0{\cdot}5)^2 T^2 [1 - 2\, e^{-\xi\omega_n \Delta t} \cos \omega_d \Delta t + (e^{-\omega_n \Delta t})^2]. \tag{4.3}$$

If $\xi \neq 0$, then B is not equal to zero.

Therefore, when $\xi \neq 0$, a two-pulse sequence which will result in damped motion with robustness cannot be found.

If $\xi = 0$, from equation (4.3) one obtains

$$B = 2a^2(L - 0{\cdot}5)^2 T^2 [1 - \cos \omega_d \Delta t] = 0$$

so that $1 - \cos(\omega_d \Delta t) = 0$, which means that $\Delta t = L'T$.

This means that, for a two-pulse sequence, it is possible to have a robust solution if the duration of the pulse is varied. However, as was mentioned earlier, such a solution may result in a very narrow pulse, and that would prevent the system from reaching its maximum velocity. Hence, in this formulation, it is assumed that the two-pulse sequence is unable to provide robustness and, instead, other pulse sequences will be used to provide the desired robustness. In the following, the result of this two-pulse sequence will be used to find the response of the system to a four-pulse and subsequently a six-pulse sequence.

4.2. DAMPED MOTION BY A FOUR- OR THREE-PULSE SEQUENCE WITH ROBUSTNESS

Consider the four-pulse sequence shown in Figure 4. It will be shown that such a sequence can be used to achieve damped motion *with robustness*. As before, one lets $k_c = e^{-\xi\omega_n t_c}$ and $k_e = e^{-\xi\omega_n t_e}$. From the previous discussion on the two-pulse sequence, it is

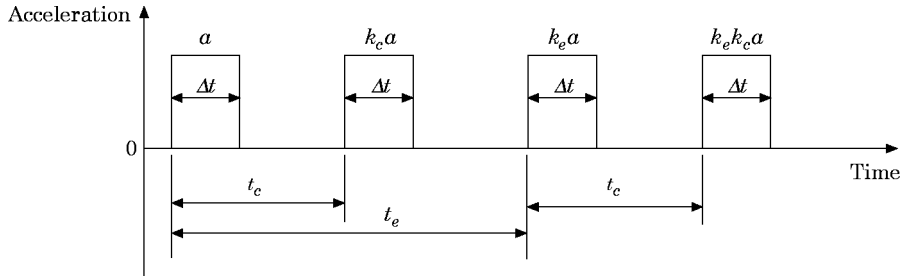

Figure 4. The acceleration profile of the four-pulse sequence for damped motion.

known that if $t_c = (L - 0{\cdot}5)T$, there will be no vibration after the second pulse and the fourth pulse. In order for the system to be robust, this four-pulse sequence should satisfy equation (3.13) to achieve zero residual vibration with robustness.

Substituting $t_c = (L - 0{\cdot}5)T$ into equation (3.13), one obtains

$$B = 4k_c^2 k_e^2 a^2 (L - 0{\cdot}5)^2 T^2 \cos^2 \omega_d \frac{t_e}{2} [1 - 2\,\mathrm{e}^{-\xi\omega_n \Delta t} \cos \omega_d \Delta t + (\mathrm{e}^{-\omega_n \Delta t})^2] = 0.$$

If $\xi \neq 0$, then since $[1 - 2\,\mathrm{e}^{-\xi\omega_n \Delta t} \cos \omega_d \Delta t + (\mathrm{e}^{-\omega_n \Delta t})^2] \neq 0$, and therefore $\cos(\omega_d t_e/2) = 0$, which means that $t_e = (L' - 0{\cdot}5)T$. If $\xi = 0$, then

$$B = 8a^2 (L - 0{\cdot}5)^2 T^2 \cos^2 \omega_d \frac{t_e}{2} [1 - \cos \omega_d \Delta t] = 0,$$

and so (a) $\cos(\omega_d t_e/2) = 0$, which means that $t_e = (L' - 0{\cdot}5)T$ where L' is an integer, or (b) $1 - \cos(\omega_d \Delta t) = 0$, which means that $\Delta t = L''T$, where L'' is an integer.

Again, as before, the solution $\Delta t = L''T$ is discarded. Hence if $t_c = (L - 0{\cdot}5)T$ and $t_e = (L' - 0{\cdot}5)T$, then the resulting system will exhibit damped motion with robustness.

A special case of this pulse sequence is when

$$t_c = (L - 0{\cdot}5)T = t_e = (L' - 0{\cdot}5)T$$

and

$$k_c = k_e = k = \mathrm{e}^{-\xi\omega_n (L - 0{\cdot}5)T}.$$

In that case, a three-pulse sequence actually resulted, as shown in Figure 5. This pulse sequence will also result in zero residual vibration with robustness. The disadvantage of this sequence is that maximum acceleration is only attained for the first or the second pulse.

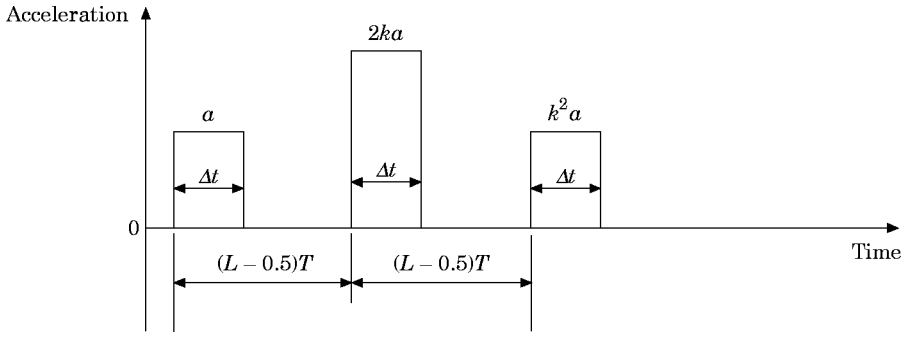

Figure 5. The acceleration profile of three-pulse sequence for damped motion.

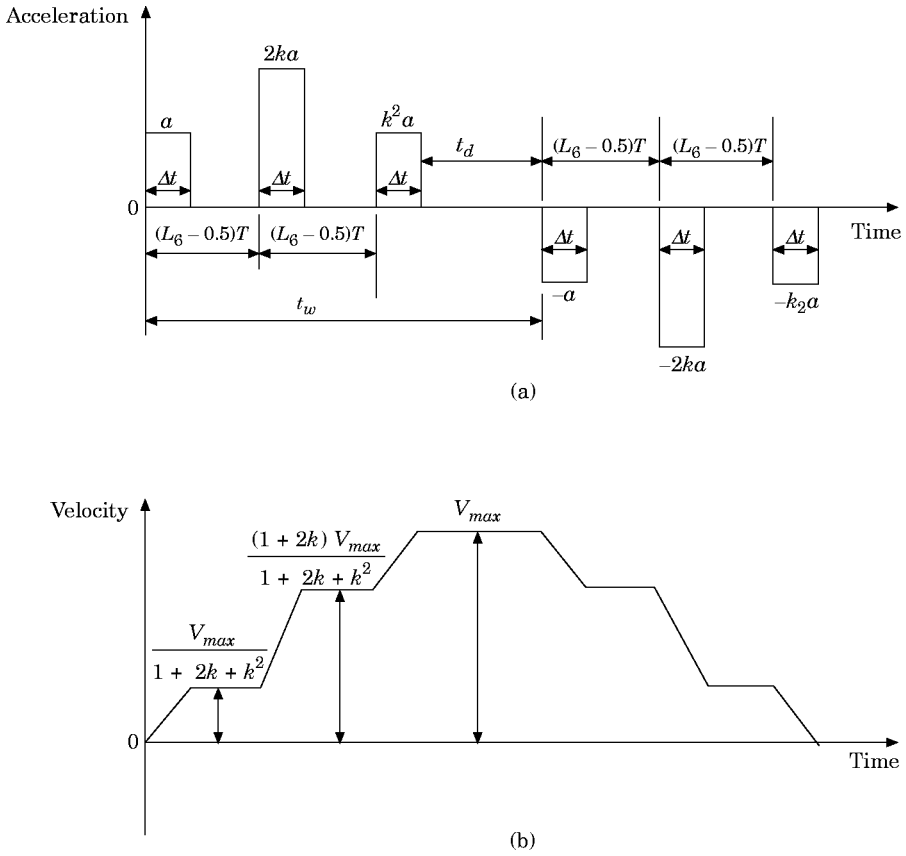

Figure 6. The proposed six-pulse sequence with robustness. (a) Acceleration profile; (b) velocity profile.

However, this pulse sequence is introduced because it is robust, can be applied to system with damping, and can be easily compared to the impulse shaper method of [12].

4.3. SIX-PULSE SEQUENCE WITH ROBUSTNESS

In the previous section, two-, three- and four-pulse sequences are shown that are able to achieve damped motion. In practice, to cause some specific rigid body motion, the rigid body velocity must start and end at zero. In that case, the forcing function must have equal positive and negative areas. Also, the optimal acceleration time history should be symmetrical about the mid-point in time. On the basis of these considerations, one can design two-pulse or four-pulse sequences for that purpose. However, it can be shown that such input sequences will not possess robustness for system with damping and hence, are of less interest. Therefore, a six-pulse sequence as shown in Figure 6(a) is introduced. From the results of section 4.2, the six-pulse sequence will result in zero residual vibration with robustness when $k = \mathrm{e}^{-\xi\omega_n (L_6 - 0{\cdot}5)T}$, with or without damping in the system. The velocity profile of this pulse sequence is shown in Figure 6(b). For the input sequence shown, the velocity of the cart at the end of the input

$$V(t_f) = a\Delta t(1 + 2k + k^2 - 1 - 2k - k^2) = 0 \tag{4.4}$$

and so it satisfies the constraint that the final velocity should be zero, so that the rigid body motion is finally at rest. It can be seen that if $t_d > 0$, there will be no vibration during the

constant velocity stage (after the third pulse) and, therefore, damped motion is achieved during that motion.

In order that the second pulse happens after the first pulse and that the time of the constant velocity stage between the first pulse and the second will be no more than one period of the system, the following constraints should be satisfied:

$$(L_6 - 0{\cdot}5 - 1)T < \Delta t \leqslant (L_6 - 0{\cdot}5)T, \tag{4.5}$$

where

$$\frac{V_{max}}{2{\cdot}25a_{max}} \leqslant \Delta t = \frac{V_{max}}{a_{max}\left(\dfrac{1}{2k} + 1 + 0{\cdot}5k\right)} \leqslant \frac{V_{max}}{2a_{max}} \qquad \text{if } 2k \geqslant 1, \tag{4.6a}$$

so that the second and the fifth pulses reach the maximum allowable acceleration and

$$\frac{V_{max}}{2{\cdot}25a_{max}} \leqslant \Delta t = \frac{V_{max}}{a_{max}\,(1 + 2k + k^2)} \leqslant \frac{V_{max}}{a_{max}}, \qquad \text{if } 2k \leqslant 1, \tag{4.6b}$$

which means that the first and the fourth pulses reach the maximum acceleration.

Using inequalities (4.5) and (4.6), it is quite easy to find the smallest integer L_6. There are two special cases that enable us to find L_6 directly.

Case (*a*):

$$\text{int}\left(\frac{V_{max}}{2{\cdot}25Ta_{max}} + 1{\cdot}5\right) = \text{int}\left(\frac{V_{max}}{Ta_{max}} + 1{\cdot}5\right).$$

From inequalities (4.6), we know that

$$\frac{V_{max}}{2{\cdot}25a_{max}} \leqslant \Delta t = \frac{V_{max}}{a_{max}\,(1 + 2k + k^2)} \leqslant \frac{V_{max}}{a_{max}},$$

and therefore

$$\text{int}\left(\frac{V_{max}}{2{\cdot}25Ta_{max}} + 1{\cdot}5\right) \leqslant L_6 \leqslant \text{int}\left(\frac{V_{max}}{Ta_{max}} + 1{\cdot}5\right). \tag{4.7a}$$

If

$$\text{int}\left(\frac{V_{max}}{2{\cdot}25Ta_{max}} + 1{\cdot}5\right) = \text{int}\left(\frac{\mathrm{V}_{\max}}{Ta_{max}} + 1{\cdot}5\right),$$

then

$$L_6 = \text{int}\left(\frac{V_{max}}{2{\cdot}25Ta_{max}} + 1{\cdot}5\right) = \text{int}\left(\frac{V_{max}}{Ta_{max}} + 1{\cdot}5\right). \tag{4.7b}$$

Case (*b*): $\xi = 0$. If $\xi = 0$, $\Delta t = V_{max}/2a_{max}$, and then from inequality (4·5) we obtain

$$L_6 = \text{int}\left(\frac{V_{max}}{2Ta_{max}} + 1{\cdot}5\right). \tag{4.7c}$$

Once L_6 is decided, then

$$k = \mathrm{e}^{-\xi w_n (L_6 - 0{\cdot}5)T} \tag{4.8}$$

and

$$\Delta t = \frac{V_{max}}{a_{max}\left(\dfrac{1}{2k} + 1 + 0{\cdot}5k\right)} \qquad \text{if } 2k \geqslant 1 \tag{4.9a}$$

or

$$\Delta t = \frac{V_{max}}{a_{max}\,(1 + 2k + k^2)} \qquad \text{if } 2k < 1. \tag{4.9b}$$

Since the distance travelled, $Z = V_{max}\, t_w$, therefore

$$t_w = Z/V_{max} \tag{4.10}$$

and

$$t_f = t_w + 2(L_6 - 0{\cdot}5)T + \Delta t. \tag{4.11}$$

Expressions (4.5), (4.7), (4.8), (4.9), (4.10) and (4.11) are used to design the six-pulse sequence to give a system with zero residual vibration with robustness for a system with or without damping.

5. SYSTEM WITHOUT PRESHAPING AND PRESHAPING USING AN IMPULSE SEQUENCE

5.1. SYSTEM WITHOUT PRESHAPING

It is well known that the time-optimal solution for a rigid body motion subjected to acceleration and velocity constraints is a rectangular or "bang–bang" input. For sufficiently long motion such that maximum velocity can be reached, the acceleration input and velocity profiles are given in Figures 7(a) and 7(b) respectively.

Using such an input profile, we have

$$\Delta t = V_{max}\,/a_{max}, \tag{5.1}$$

and

$$t_w = Z/V_{max} \tag{5.2}$$

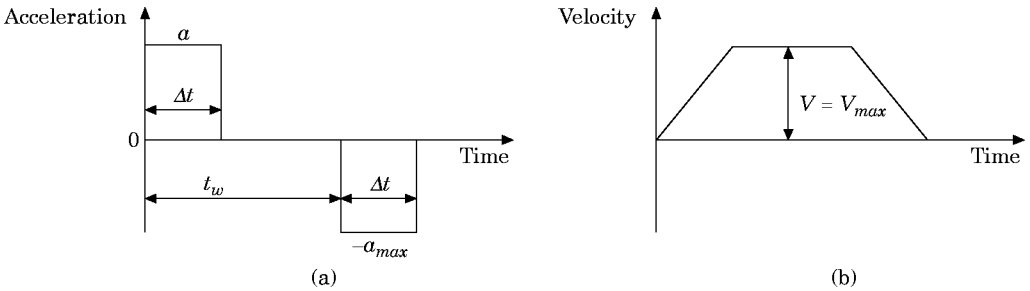

Figure 7. "Bang–bang" input. (a) Acceleration profile; (b) velocity profile.

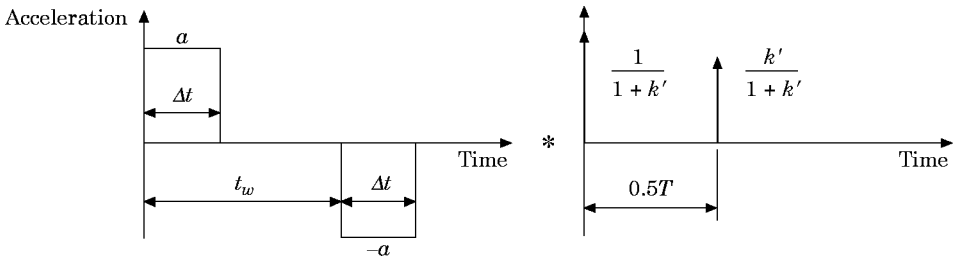

Figure 8. The impulse shaper method without robustness.

where, as before, Z is the distance of the desired motion. Then, the total time taken for the rigid body motion is

$$t_f = t_w + \Delta t = \frac{Z}{V_{max}} + \frac{V_{max}}{a_{max}}. \tag{5.3}$$

Since vibration is not considered, such input is the theoretically fastest time taken to complete a motion. Of course, since the vibration is not handled, the resulting motion will cause residual vibration in most cases.

5.2. PRESHAPING USING AN IMPULSE SEQUENCE

Singer and Seering [12] have developed an elegant impulse shaper method to reduce system vibration. They use a two-impulse sequence as shown in Figure 8 for the non-robust case, and a three-impulse sequence as shown in Figure 9 for the robust case (where $k' = e^{-0.5\xi\omega_n T}$). The impulse sequences are not used to drive the system directly. Instead, they are convolved with a rigid body acceleration profile as shown in Figure 7(a) to generate new acceleration profile that is used to drive the system. The resulting system after convolution will result in the same distance travelled with the same end velocity as the original desired rigid body motion, but with substantially reduced residual vibration.

From Figure 9, the time taken to complete the motion for the impulse shaper with robustness is given by

$$t_f^2 = t_w + T + \Delta t = \frac{Z}{V_{max}} + T + \frac{V_{max}}{a_{max}}. \tag{5.4}$$

Looking at Figure 9, it can be seen that the shape of the input is similar to the six-pulse sequence with robustness in section 4.3. Compared with the six-pulse sequence in

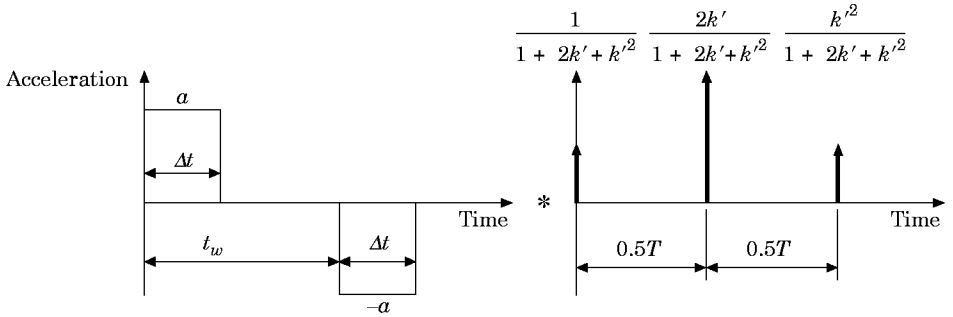

Figure 9. The impulse shaper method with robustness.

section 4.3, if one denotes the time taken for the six-pulse sequence with robustness as t_f^6, then

$$t_f^2 - t_f^6 = -2(L_6 - 1)T + \left(1 - \frac{1}{1 + 2k + k^2}\right)\frac{V_{max}}{a_{max}} \qquad \text{if } 2k < 1, \tag{5.5a}$$

$$t_f^2 - t_f^6 = -2(L_6 - 1)T + \left(1 - \frac{1}{1/2k + 1 + 0{\cdot}5k^2}\right)\frac{V_{max}}{a_{max}} \qquad \text{if } 2k \geqslant 1. \tag{5.5b}$$

If $L_6 = 1$, then the time difference is

$$t_f^2 - t_f^6 = \left(1 - \frac{1}{1 + 2k + k^2}\right)\frac{V_{max}}{a_{max}} \qquad \text{if } 2k < 1, \tag{5.6a}$$

$$t_f^2 - t_f^6 = \left(1 - \frac{1}{1/2k + 1 + 0{\cdot}5k^2}\right)\frac{V_{max}}{a_{max}} \qquad \text{if } 2k \geqslant 1. \tag{5.6b}$$

In this case, the proposed method results in a shorter time. If one modifies the six-pulse sequence with robustness developed in section 4.3 by letting $L_6 = 1$ and multiplying the height of every pulse by a factor of $1/(1 + 2k + k^2)$ when $2k < 1$ or a factor of $1/(1/2k + 1 + 0{\cdot}5k^2)$ when $2k \geqslant 1$, then the pulse sequence developed in section 4.3 is exactly the same as the impulse shaper with robustness.

6. SIMULATION RESULTS AND DISCUSSION

In order to illustrate the effectiveness, robustness and efficiency of the pulse sequences developed, some simulation results for the system are given. In addition to finding the time taken for a move, other useful parameters such as the maximum vibration during the movement Δx_{max} ($\Delta x_{max} = \max_{0 \leqslant t \leqslant t_f} |\Delta x(t)|$) and the mean vibration during the movement, $\Delta\bar{x}$ ($\Delta\bar{x} = (1/t_f)\int_0^{t_f} |\Delta x(t)| \mathrm{d}t$) are also found.

In the simulations, the system with damping will be considered. The system parameters used are as follows: natural frequency, $\omega_n = 1{\cdot}571$ rad/s; damping ratio $\xi = 0{\cdot}05$; maximum acceleration, $a_{max} = 0{\cdot}5$ m/s^2; and desired distance moved, $Z = 2{\cdot}75$ m. Two types of proposed inputs are designed, the four-pulse without robustness and the six-pulse with robustness. The inputs $u(t)$ m/s^2, the corresponding velocity profile $v(t)$ m/s, the position $z(t)$ m and the vibration $\Delta x(t)$ m for the two cases are plotted in Figures 10 and 11. For comparison, the inputs and responses of the impulse shaper method by Singer and Seering [12] without and with robustness are plotted in Figures 12 and 13 respectively. The times taken to complete the motion, mean vibration and maximum vibration of all the methods are shown in Table 1.

To compare the efficiency of these pulse sequences with varying distance Z and damped period T, the total time taken using these pulse sequences is plotted against Z and T and given in Figures 14 and 15 respectively. The difference in the time taken between the proposed methods and the impulse shaper method, for a varying damping ratio, is shown in Figure 16.

The next set of simulations is carried out to give an indication of the robustness of the proposed pulse sequences. Simulations are carried out assuming errors in the natural frequency (ω_n) used in the controller designs as compared to the actual natural frequency of the system ω_a. In Figure 17 is shown the maximum amplitude of residual vibration,

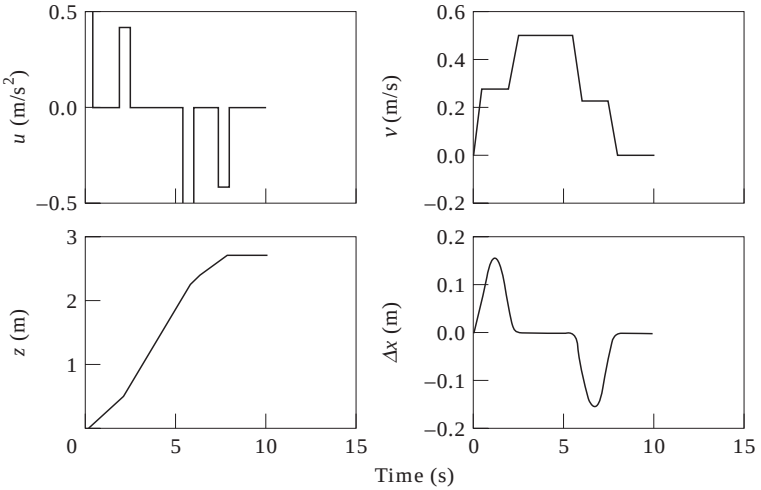

Figure 10. The input and response of the proposed four-pulse sequence without robustness.

E_{max} ($E_{max} = \max_{t \geq t_f} |\Delta x(t)|$) plotted against the ratio of the ω_a / ω_n for up to 20% error in the estimated natural frequency. As expected, the plots of the proposed pulse sequences, as well as the impulse shaper's method, are "notch-like" for the non-robust cases and much "flatter" for the robust cases. This indicates that the robust cases are much more insensitive to modelling errors.

The above simulations clearly demonstrate that the proposed pulse sequences can move the system without causing residual vibration when the model is exact and with very little residual vibration when the model is not known exactly. In the latter case, pulse sequences with robustness should be used. Although one can improve the insensitivity by constraining the pulse sequence to satisfy the robustness conditions, one should also know that, with the same system parameters, the pulse sequence that is more insensitive to errors in the natural frequency or the damping ratio takes a longer time to finish the given task.

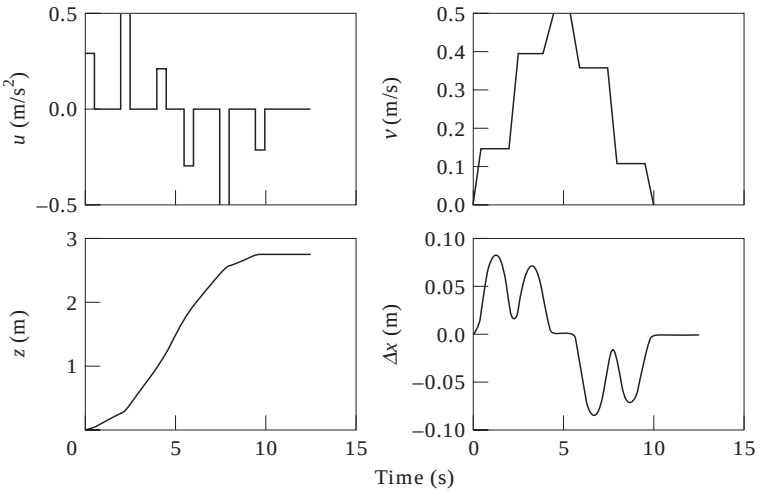

Figure 11. The input and response of the proposed six-pulse sequence with robustness

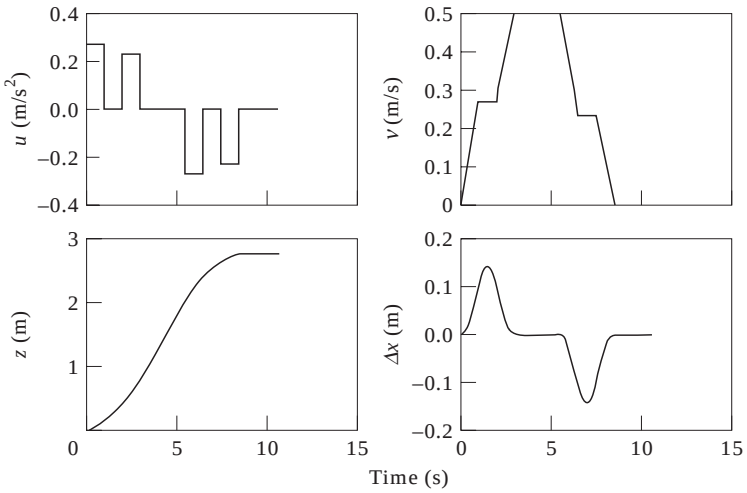

Figure 12. The input and response of the impulse shaper method without robustness.

Therefore, there is a trade-off between the shortest total time taken and the insensitivity of a pulse sequence.

7. EXPERIMENTAL RESULTS

7.1. THE SYSTEM SET-UP

To verify the effectiveness of our pulse sequences, some experiments were carried out on a model of an overhead crane. This consists of a platform (cart) mounted on a motorized linear guide moving in the horizontal direction with a cable and point load attached. The platform is controlled by a IBM-compatible 486 computer in a closed loop fashion, with encoder feedback to obtain the position of the cart. The experimental set-up of the crane system is shown in Figure 18, and the block diagram for the computer-controlled crane system is shown in Figure 19.

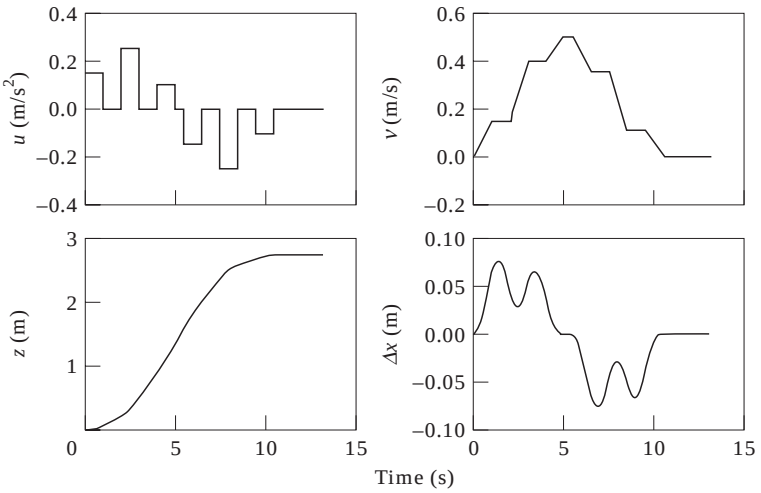

Figure 13. The input and response of the impulse shaper method with robustness.

TABLE 1

Comparison of proposed and impulse shaper method with $\xi = 0{\cdot}05$

		Time taken, t_f (s)	Mean vibration, $\Delta\bar{x}$ (m)	Maximum vibration, Δx_{max} (m)
1	Four-pulse sequence without robustness	8·0	0·050	0·154
2	Six-pulse sequence with robustness	10·0	0·040	0·084
3	Impulse shaper method without robustness	8·5	0·047	0·143
4	Impulse shaper method with robustness	10·5	0·038	0·077

The oscillation or vibration of the point load is obtained using a Hamamatsu PSD (Position Sensitive Detector). The PSD is an optoelectronic sensor that provides continuous position data of the light spot travelling over its photosensitive surfaces. The detector of the PSD is mounted on the cart, and the light source of the PSD is attached at the end-point of the cable. When the light source attached to the cable vibrates with the cable, there will be a voltage output from the PSD. The output is then sampled by an AD converter and stored in the computer.

7.2. THE EXPERIMENTAL RESULTS

In the experiment, the acceleration pulse sequence is designed and converted to the desired displacement profile by double integration. The displacement profile thus obtained is then fed into the computer-controlled crane system as the reference input. The actual displacement of the cart and the vibration are sampled and stored in the computer. By differentiating the actual displacement profile with respect to time, the velocity profile can be found; and by differentiating the actual velocity profile with respect to time, the acceleration profile is obtained.

The system natural frequency and damping ratio are experimentally determined and found to be $\omega_n = 4{\cdot}241$ rad/s, while the damping ratio $\xi = 0$. The other parameters of this system due to the limitations of the motor and/or setup are as follows: $a_{max} = 1{\cdot}0\ \text{m/s}^2$,

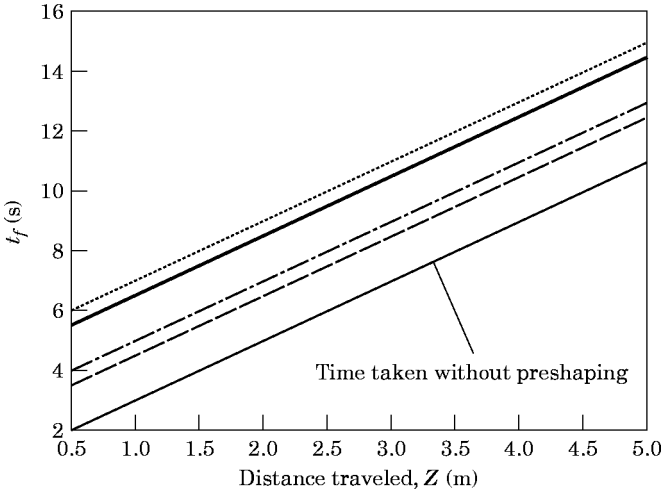

Figure 14. The total time taken t_f versus distance Z for the different methods. — —, Four-pulse sequence (non-robust); ——, six-pulse sequence (robust); — · —, impulse shaper (non-robust); ·····, impulse shaper (robust); —, no preshaping.

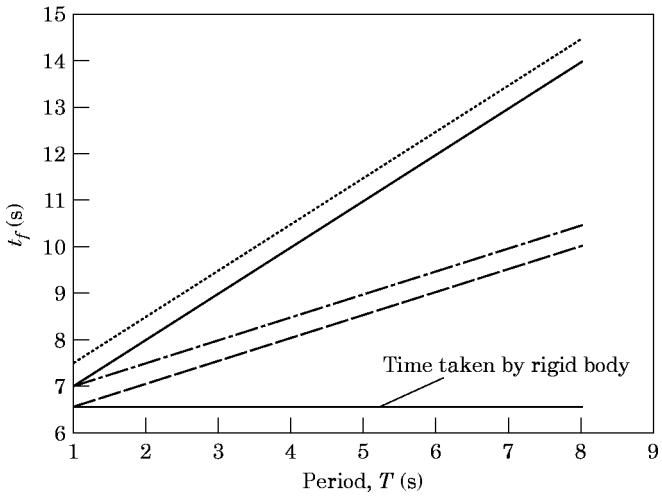

Figure 15. The total time taken versus damped period T for the different methods. — —, Four-pulse sequence (non-robust); ——, six-pulse sequence (robust); — · —, impulse shaper (non-robust); ·····, impulse shaper (robust); —, no preshaping.

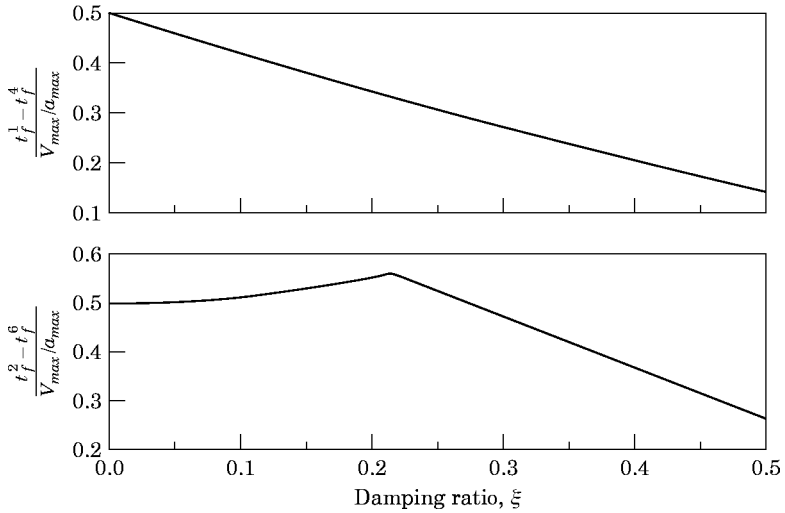

Figure 16. The time difference between the proposed methods and the impulse shaper method versus the damping ratio ξ when $L_4 = 1$ and $L_6 = 1$.

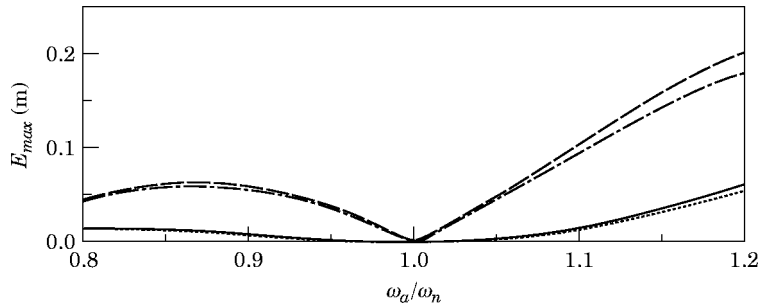

Figure 17. The maximum amplitude of residual vibration E_{max} versus ω_a/ω_n for the various methods. — —, Four-pulse sequence (non-robust); ——, six-pulse sequence (robust); — · —, impulse shaper (non-robust); ·····, impulse shaper (robust).

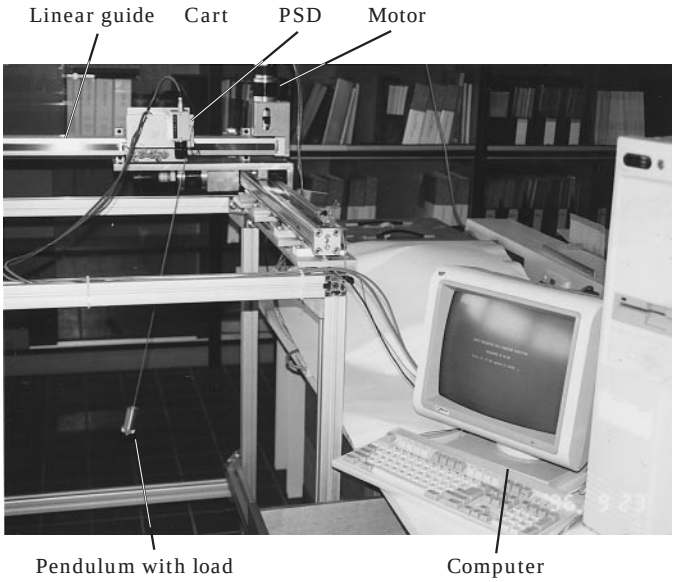

Figure 18. The experimental set-up of an overhead crane system.

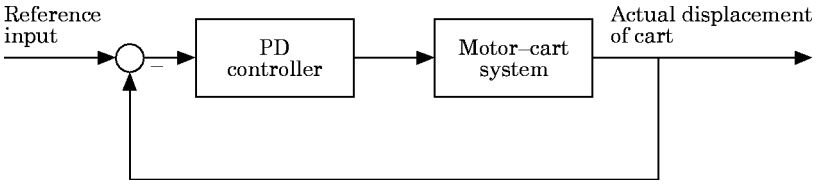

Figure 19. The block diagram for the computer-controlled platform (cart).

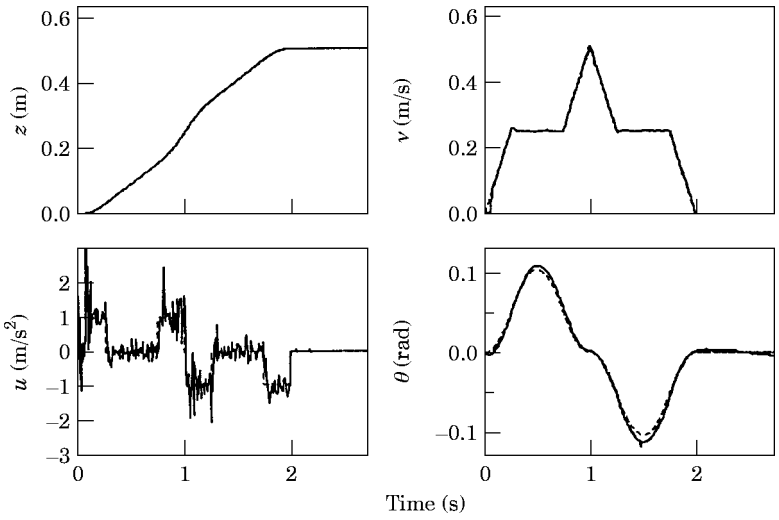

Figure 20. The input and response of the proposed four-pulse sequence when $\omega_n = \omega_a$ (i.e., the actual and design natural frequencies are equal).

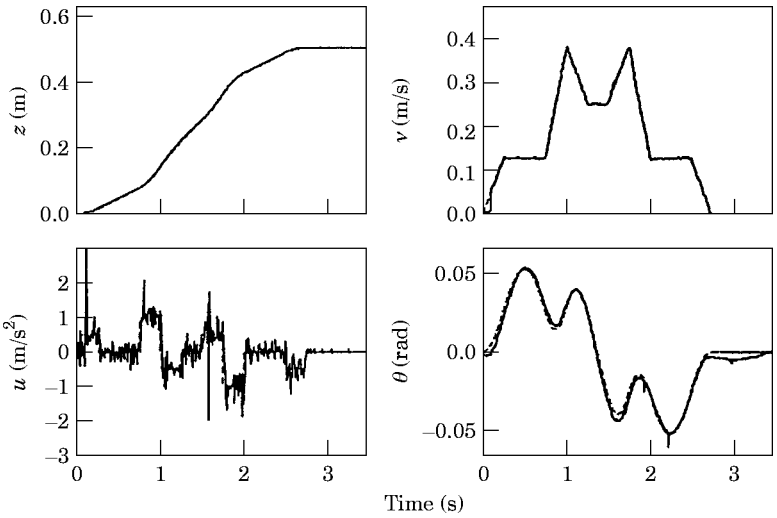

Figure 21. The input and response of the proposed six-pulse sequence when $\omega_n = \omega_a$ (i.e., the actual and design natural frequencies are equal).

$V_{max} = 0{\cdot}5$ m/s, $Z = 0{\cdot}5$ m. All of the pulse sequences are designed according to this set of parameters. In the subsequent plots of the results, the theoretical results are represented by the dashed lines and the experimental results are represented by the solid lines.

In the first set of experiments, the actual natural frequency of the system found by experiment is used in the design of the pulse sequences. This means that the system model is exact and no intentional modelling errors are introduced. Two types of input sequences—namely, the four-pulse sequence without robustness and the six-pulse sequence with robustness—are used. The plots of the position of the cart, $z(t)$ m, the velocity profile $v(t)$ m/s, the acceleration $u(t)$ m/s^2 and the vibration of the end-point $\theta(t)$ rad for the four types of inputs are shown in Figures 20 and 21 respectively. It can be seen from the figures that the theoretical displacement profile and the experimental displacement profile of the cart are so close that it is almost impossible to distinguish the differences. The experimental velocity profile and the acceleration profile, however, contain some noise, which is understandable because they are obtained through differentiation. It is clear from the figures that residual vibration after the motion is almost non-existent. It is also observed that damped motion is achieved for the four pulse sequence without robustness, and the six pulse sequence with robustness, as was designed. The experimentally determined maximum vibration during motion ($\theta_{max} = \max_{0 \leqslant t \leqslant t_f} |\theta(t)|$) and the time taken for the motion are given in Table 2.

In order to illustrate the robustness of the proposed pulse sequences, the next set of experiments were performed using an erroneous estimate of the system model. Here, by

TABLE 2

Experimental results using proposed input sequences

		Time taken, t_f (s)	Maximum vibration, θ_{max} (rad)
1	Four-pulse sequence without robustness	1·991	0·112
2	Six-pulse sequence with robustness	2·731	0·0526

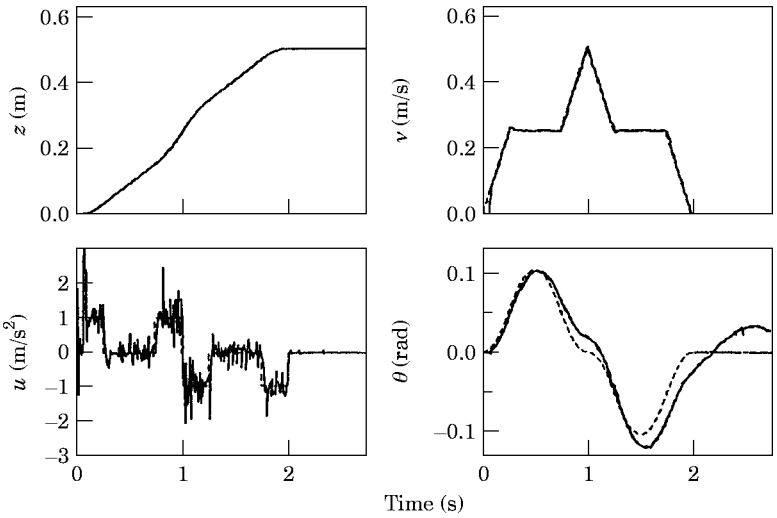

Figure 22. The input and response of the proposed four-pulse sequence when $\omega_n \neq \omega_a$ (i.e., there is an error in the actual and design natural frequencies).

changing the length of cable, the natural frequency of the actual system was changed to $\omega_a = 3{\cdot}980$ rad/s, which is about 6% less than the design frequency ($\omega_n = 4{\cdot}241$ rad/s). The pulse sequence designed by using $\omega_n = 4{\cdot}241$ rad/s was then used to drive the system, the actual frequency of which ω_a was 3·980 rad/s. In Figures 22 and 23 are shown the theoretical and experimental results or our proposed pulse sequences when there is an error in system design frequency (or modelling frequency) for the four-pulse without robustness and the six-pulse with robustness. It can be seen that the six-pulse sequence with robustness results in very little residual vibration, while the residual vibrations caused by the four-pulse sequence without robustness are relatively large. The experimentally determined maximum residual vibration for the various inputs is shown in Table 3.

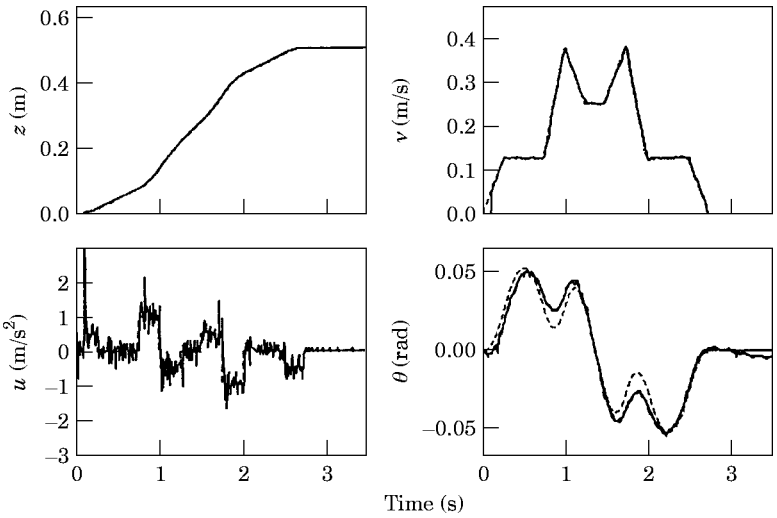

Figure 23. The input and response of the proposed six-pulse sequence when $\omega_n \neq \omega_a$ (i.e., there is an error in the actual and design natural frequencies).

TABLE 3

Amplitude of maximum residual vibration using proposed input sequences

		Maximum residual vibration, E_{max} (rad)
1	Four-pulse sequence without robustness	0·040
2	Six-pulse sequence with robustness	0·005

The experiments show that the maximum amplitude of the residual vibration is reduced significantly (by an order of magnitude) for the pulse sequences with robustness as compared to the pulse sequence without robustness when there are modelling errors. This means that while the pulse sequences without robustness can be sensitive to the change or shift of the system natural frequency (or damping ratio), the pulse sequences with robustness are quite insensitive to the change or shift of the system natural frequency (or damping ratio).

8. CONCLUSIONS

In this paper, it is shown that the use of pulse sequences as the shaped input for a single-mode flexible system can significantly reduce the residual vibration while causing the rigid body to perform a desired motion. It is also shown that some of the pulse sequences developed possess some robustness to variations in the natural frequencies and damping ratios of the systems. Inputs in the form of a four-pulse sequence without robustness and a six-pulse sequence are developed. The shaped input method developed here is straightforward and do not require measurements of the system's states. Hence, it is direct and easier to implement on actual systems. Simulations and experiments show that the proposed method is easy to design and effective in implementation.

REFERENCES

1. R. H. CANNON, JR. and E. SCHMITZ 1984 *The International Journal of Robotics Research* **3**, 325–338. Initial experiments on the end-point control of a flexible one-link robot.
2. P. T. KOTNIK, S. YURKOVICH and U. OZGUNER 1988 *Journal of Robotic Systems* **5**, 181–196. Acceleration feedback for control of a flexible manipulator arm.
3. K. KUO and D. WANG 1992 *Proceedings of the IEEE International Conference on Robotics and Automation* **1**, 782–787. Closed loop shaped-input control of a class of manipulators with a single flexible link.
4. D. P. MAGEE and W. J. BOOK 1993 *Proceedings of the IEEE International Conference on Robotics and Automation* **2**, 474–479. Eliminating multiple modes of vibration in a flexible manipulator.
5. O. J. M. SMITH 1958 *Feedback Control Systems*. New York: McGraw-Hill. See pp. 331–345.
6. O. J. M. SMITH 1957 *Proceedings of the Institute of Radio Engineers* **45**, 1249–1255. Posicast control of damped oscillatory systems.
7. D. M. ASPINWALL 1980 *Journal of Dynamic Systems*, *Measurement*, *and Control* **102**, 3–6. Acceleration profiles for minimizing residual response.
8. R. L. FARRENKOF 1979 *American Institute of Aeronautics and Astronautics*, *Journal of Guidance and Control* **2**, 491–498. Optimal open-loop maneuver profiles for flexible spacecraft.
9. C. J. SWIGERT 1980 *American Institute of Aeronautics and Astronautics*, *Journal of Guidance and Control* **3**, 460–467. Shaped torque techniques.
10. P. H. MECKLE and R. KINCELER, 1994 *IEEE Transactions on Control Systems Technology* **2**, 245–254. Robust motion control of flexible systems using feedforward forcing functions.
11. J. F. JONES, B. J. PETTERSON and J. C. WERNER 1990 *Sandia Report* (*Sand*87-2189 *UC*-406), *Sandia National Laboratories*. Swing damped movement of suspended objects.
12. N. C. SINGER and W. P. SEERING 1990 *Journal of Dynamic Systems*, *Measurement*, *and Control* **112**, 76–82. Preshaping command inputs to reduce system vibration.